

Review

## Limited proteolysis in the investigation of $\beta$ 2-microglobulin amyloidogenic and fibrillar states

M. Monti <sup>a</sup>, A. Amoresano <sup>b</sup>, S. Giorgetti <sup>c,d</sup>, V. Bellotti <sup>c,d</sup>, P. Pucci <sup>a,b,\*</sup>

<sup>a</sup> CEINGE Biotecnologie Avanzate, scarl, Università di Napoli Federico II, Via Comunale Margherita 482, 80145 Napoli, Italy

<sup>b</sup> Dipartimento di Chimica Organica e Biochimica, Università di Napoli Federico II, Via Cinthia 6, 80125 Napoli, Italy

<sup>c</sup> Dipartimento di Biochimica, Università di Pavia, via Taramelli 3b, 27100 Pavia, Italy

<sup>d</sup> Laboratorio di Biotecnologie, IRCCS Policlinico S. Matteo, p.le Camillo Golgi 2, 27100 Pavia, Italy

Received 6 July 2005; received in revised form 26 August 2005; accepted 8 September 2005

Available online 23 September 2005

### Abstract

Amyloid fibrils of patients treated with regular haemodialysis essentially consists of  $\beta$ 2-microglobulin ( $\beta$ 2-m) and its truncated species  $\Delta$ N6 $\beta$ 2-m lacking six residues at the amino terminus. The truncated fragment shows a higher propensity to self-aggregate and constitutes an excellent candidate for the analysis of a protein in the amyloidogenic conformation. The surface topology and the conformational analysis of native  $\beta$ 2-m and the truncated  $\Delta$ N6 $\beta$ 2-m species both in the soluble and in the fibrillar forms were investigated by the limited proteolysis/mass spectrometry strategy. The conformation in solution of a further truncated mutant  $\Delta$ N3 $\beta$ 2-m lacking three residues at the N-terminus was also examined. This approach appeared particularly suited to investigate the regions that are solvent-exposed, or flexible enough to be accessible to protein–protein interactions and to describe the conformation of transient intermediates. Moreover, proteolysis experiments can also be tailored to investigate amyloid fibrils by discriminating the protein regions constituting the unaccessible core of the fibrils and those still flexible and exposed to the solvent. Although native  $\beta$ 2-m and  $\Delta$ N3 $\beta$ 2-m shared essentially the same conformation, significant structural differences exist between the native and the  $\Delta$ N6 $\beta$ 2-m proteins in solution with major differences located at the end moiety of strand V and subsequent loop with strand VI and at both the N- and C-termini of the proteins. On the contrary, an identical distribution of preferential proteolytic sites was observed in both proteins in the fibrillar state, which was nearly superimposable to that observed for the soluble form of  $\Delta$ N6 $\beta$ 2-m. These data revealed that synthetic fibrils essentially consists of an unaccessible core comprising residues 20–87 of the  $\beta$ 2-m protein with exposed and flexible N- and C-terminal ends. Moreover, proteolytic cleavages observed *in vitro* at Lys 6 and Lys 19 reproduce specific cleavages that have to take place *in vivo* to generate the truncated forms of  $\beta$ 2-m occurring in natural fibrils. On the basis of these results, a molecular mechanism for fibril formation has been proposed.

© 2005 Elsevier B.V. All rights reserved.

**Keywords:** Amyloid fibril;  $\beta$ 2-microglobulin; Limited proteolysis; Mass spectrometry

### 1. Introduction

The investigation of the mechanism of amyloid fibrils formation by globular proteins is focused on the isolation and structural characterization of intermediates of the unfolding pathway that self aggregate in ordered fibrillar structures [1]. In this respect, the term amyloidogenic conformation is used to indicate the conformation that a protein should acquire,

even transiently, to fit properly within the fibrillar template. In spite of its relevance, the investigation of protein aggregation at a residue level is technically challenging essentially because of the instability of the transient intermediates which are generated during the aggregation process. Atomic force microscope [2], NMR [3,4] and X-ray diffraction [5] have shed light on the overall structure of the soluble and fibrillar states, but could not provide detailed information about intra- and intermolecular interactions of the protein monomer within the fibrils. Moreover, they were not able to describe the conformational changes occurring in the protein structure during the conversion from the native form to the fibrillar state.

\* Corresponding author. Dipartimento di Chimica Organica e Biochimica, Università di Napoli Federico II, Via Cinthia 6, 80125 Napoli, Italy. Tel.: +39 813722896/81674318; fax: +39 813722808/081674313.

E-mail address: [pucci@unina.it](mailto:pucci@unina.it) (P. Pucci).

Systematic protein engineering approaches, in which single residues are substituted or deleted one by one, provided detailed information on the regions of the sequence that are involved in the rate-determining steps of aggregation. [6–9]. Nevertheless, they are not able to clarify the precise mechanism of aggregation, nor the structure of the amyloidogenic monomeric state or the resulting aggregates.

A systematic approach of limited proteolysis experiments in combination with mass spectrometry constitutes an alternative and complementary strategy to investigate the protein regions that are solvent-exposed, or flexible enough to be accessible to protein–protein interactions. The native conformation of proteins, in fact, provides some stereochemical barriers to enzymatic attack, leaving the exposed and flexible regions accessible to proteases and preventing the occurrence of proteolytic cleavages within the highly structured core of the protein molecule, or at least slowing their kinetics. Although exposed side chains might be non-susceptible to protease cleavage for a number of reasons, the identification of the peptide bonds most sensitive to enzymatic hydrolysis is strongly indicative of the amino acid residues located at the protein surface. The peptide bonds susceptible to protease action and hence the accessible amino acid residues are assigned from the identification of the two complementary peptides released from the intact protein following a single proteolytic event, as shown in Fig. 1. Consequently, when these experiments are performed using a series of proteases with different specificities, the pattern of preferential cleavage sites can identify the exposed regions of the protein [10].

This procedure is ideally suited to monitor conformational changes occurring in protein structure in passing from the native state to the amyloidogenic intermediates and to identify the regions involved in the variations. Since the surface topology of the protein is affected by conformational changes, when comparative experiments are carried out on both the native protein and the amyloid intermediates differential proteolytic site maps are obtained from which the protein regions involved in the structural changes can be inferred (Fig. 2) [11].

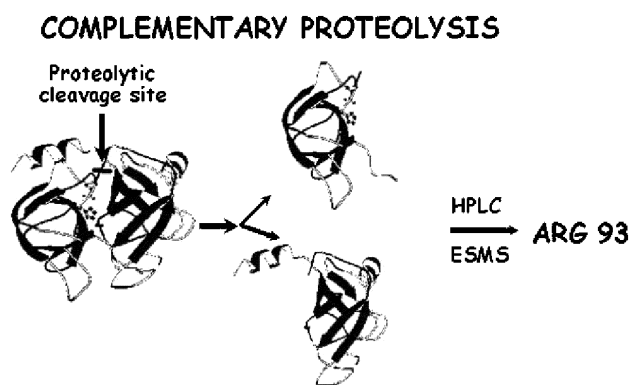


Fig. 1. Identification of the preferential cleavage sites in the limited proteolysis mass spectrometry approach. Accessible amino acid residues were assigned from the identification of the two complementary peptides released from the intact protein following a single proteolytic event through the determination of their accurate molecular masses.

Moreover, proteolysis experiments can also be tailored to investigate amyloid fibrils, as the distribution of proteolytic sites can lead to a description of the protein regions constituting the unaccessible core of the fibrils and those still flexible and exposed to the solvent.

Identification of the cleavage sites within the protein structure during limited proteolysis experiments carried out on a time-course basis needs a rapid, sensitive and definitive analytical methodology. In this respect, advanced mass spectrometric procedures seem to fulfill these prerequisites and represent an ideal approach to effectively analyze fragments enzymatically released from the native protein leading to unambiguous identification of the protease sensitive sites [10].

The limited proteolysis/mass spectrometry approach was employed in the structural characterization of the amyloidogenic state of the human  $\beta 2$ -microglobulin, ( $\beta 2$ -m) associated with a type of amyloidosis, DRA, which represents an inevitable and severe complication of long-term haemodialysis [12]. Natural amyloid fibrils of patients with chronic renal failure treated with regular haemodialysis contains both full-length  $\beta 2$ -microglobulin ( $\beta 2$ -m) as well as some proteolytically processed fragments [13], with the main truncated species lacking 6 ( $\Delta N6\beta 2$ -m) and 19 ( $\Delta N19\beta 2$ -m) residues at the amino terminus, respectively. The proteolytic removal of the first six N-terminal residues occurs at 30% of the  $\beta 2$ -m molecules extracted from ex vivo fibrils [14]. This truncated species was shown to have a higher tendency to self-aggregate than the full-length protein.  $\Delta N6\beta 2$ -m is able to rapidly generate amyloid fibrils even at physiological pH and did not form a fully folded native state at the end of the refolding procedure [14]. This truncated species still has a certain level of three-dimensional structure and shows a minimal energetic barrier for fibril formation thus constituting an excellent candidate for the determination of the surface topology of a protein in the amyloidogenic conformation.

The surface topology and the conformational analysis of native  $\beta 2$ -m and the  $\Delta N6\beta 2$ -m truncated species both in soluble and in the fibrillar forms were investigated by the limited proteolysis/mass spectrometry methodology. The conformation in solution of a further truncated mutant  $\Delta N3\beta 2$ -m lacking three residues at the N-terminus was also examined.

## 2. Materials and methods

### 2.1. Samples preparation

Native  $\beta 2$ -m and the truncated  $\Delta N3\beta 2$ -m and  $\Delta N6\beta 2$ -m proteins were obtained by recombinant DNA methodologies as previously described [16]. Fibrils from both intact and  $\Delta N6\beta 2$ -m were prepared at pH 4 and separated from soluble  $\beta 2$ -m species by centrifugation in ultracentrifuge at 10,000 rpm. The pellet was washed extensively and finally resuspended in the optimum buffer to perform the limited proteolysis experiments [18].

### 2.2. Limited proteolysis experiments

Limited proteolysis experiments were carried out by incubating soluble  $\beta 2$ -m and the truncated species with trypsin, endoprotease AspN, endoprotease V8, chymotrypsin, proteinase K and elastase. Insoluble protein fibrils were treated

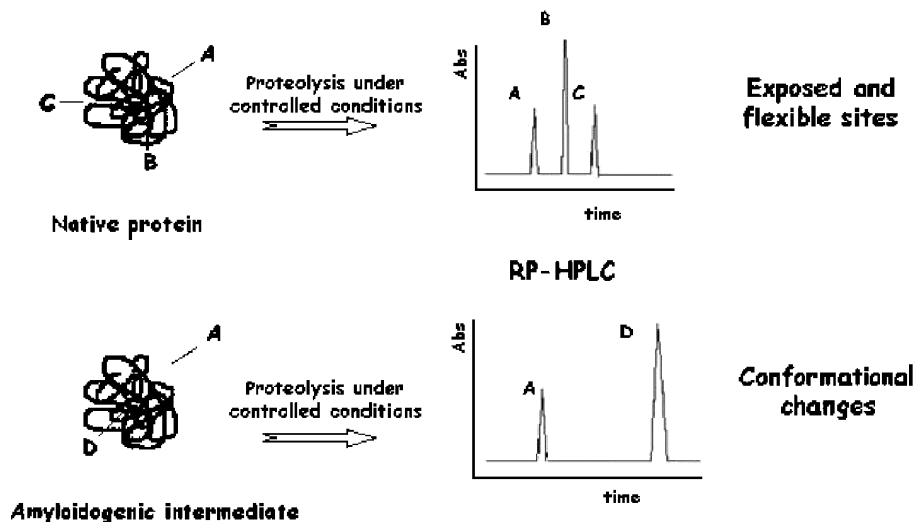


Fig. 2. Schematic description of the limited proteolysis mass spectrometry strategy applied to the investigation of conformational changes in the formation of amyloidogenic intermediates.

with trypsin, chymotrypsin, and endoprotease AspN. Enzymatic digestions were all performed in 100 mM sodium phosphate (pH 7.5) at 37 °C using enzyme-to-substrate ratios ranging between 1:5 and 1:700 (w/w) for the soluble forms and 1:100 and 1:1000 (w/w) for the fibrils. The persistence of fibrils at this pH in the interval of proteolytic digestion was monitored by the Thioflavin assay. No differences in specific fluorescence of the thioflavin–fibrils complex was found in buffer at pH 4 or 7.5. The extent of the reaction was monitored on a time-course basis by sampling the incubation mixture at different time intervals and dissolving the remaining aggregates in 40% acetonitrile containing 0.4% TFA.

### 2.3. Chromatographic separation of peptides

Peptide mixtures from the different proteolysis experiments were fractionated by reverse-phase HPLC on a Phenomenex Jupiter C18 column 250 × 2.1 mm, 300 Å pore size) with a linear gradient from 5% to 50% acetonitrile in 0.1% trifluoroacetic acid (TFA) over 40 min, at a flow rate of 200 µL/min; elution was monitored at 220 nm. Individual fractions were manually collected and identified by ESMS.

### 2.4. Mass spectrometry

Proteolytic fragments were analyzed by electrospray MS using an API-100 single quadrupole instrument (Applied Biosystem). Samples were injected directly into the ion source by a Harvard syringe pump at a flow rate of 3 µL/min. Data were acquired and processed by the Biomultiviewer software provided by the manufacturer. The instrument was calibrated by a separate injection of horse heart myoglobin (average molecular mass 16,951.5 Da); all masses are reported as average mass.

When necessary, identification of disulphide-bridged peptides was carried out by reduction of the samples with 10 mM dithiothreitol in 50 mM Tris–HCl, 1 mM EDTA (pH 7.5), containing 6 M GdnHCl, for 2 h at 37 °C under nitrogen, followed by MALDI mass spectrometry (MALDI/MS) analysis using a Voyager DE instrument (Applied Biosystem). Typically, 1 µL of analyte solution was mixed with 1 µL of  $\alpha$ -cyano-4-hydroxycinnamic acid 10 mg/mL in acetonitrile/0.2% TFA, 70:30 v/v, containing 250 fmol of bovine insulin. The mixture was applied onto the metallic sample plate and air dried. Mass calibration was performed using the quasi-molecular ions of insulin at  $m/z$  5734.5 and a matrix peak at  $m/z$  379.1. All mass values are reported as average masses.

## 3. Results

The surface topology of soluble  $\beta$ 2-m and its N-terminal truncated species,  $\Delta$ N3 $\beta$ 2-m and  $\Delta$ N6 $\beta$ 2-m was investigated

by the limited proteolysis/mass spectrometry approach. Moreover, amyloid fibrils obtained *in vitro* from native  $\beta$ 2-m and  $\Delta$ N6 $\beta$ 2-m were also examined. These experiments aimed to investigate conformational changes affecting protein topology in the transition from the soluble state to the fibrils and to gain insight into the fibril structure by monitoring the appearance/disappearance of preferential cleavage sites.

### 3.1. Limited proteolysis on soluble $\beta$ 2-m, $\Delta$ N3 $\beta$ 2-m and $\Delta$ N6 $\beta$ 2-m

Limited proteolysis experiments were performed on recombinant  $\beta$ 2-m and the truncated forms  $\Delta$ N3 $\beta$ 2-m and  $\Delta$ N6 $\beta$ 2-m at a protein concentration of 10 µM. At this protein concentration, all the proteins showed the same retention time by gel filtration, consistent with the presence of monomers and dimers. The experiments were performed using several different proteases (trypsin, endoprotease AspN, endoprotease V8, chymotrypsin, proteinase K and elastase) with the aim to create conditions in which the selectivity of the cleavage was not related to, or limited by, the specificity of the enzyme. For each protease, the appropriate enzyme/protein ratio was accurately determined to generate a limited number of proteolytic events and to address protease action towards the most flexible and solvent-exposed sites. Peptide fragments released from each experiment were separated by reverse-phase HPLC and identified by ESI MS. This allowed the positions of the cleavage sites to be assigned.

As an example, Fig. 3A shows the HPLC analysis of the endoprotease Asp-N digest of native  $\beta$ 2-m after 15 min of reaction. Two components displaying molecular masses of  $11200.1 \pm 1.5$  Da and  $11877.6 \pm 1.0$  Da were detected in the early stages of digestion (fractions 1 and 2 respectively). These species were tentatively assigned to fragments (1–52)+(59–99) joined by the  $\beta$ 2-m S–S bridge and to a nicked form of the protein, respectively. Reduction of these fragments with dithiothreitol followed by MALDI/MS analysis revealed the

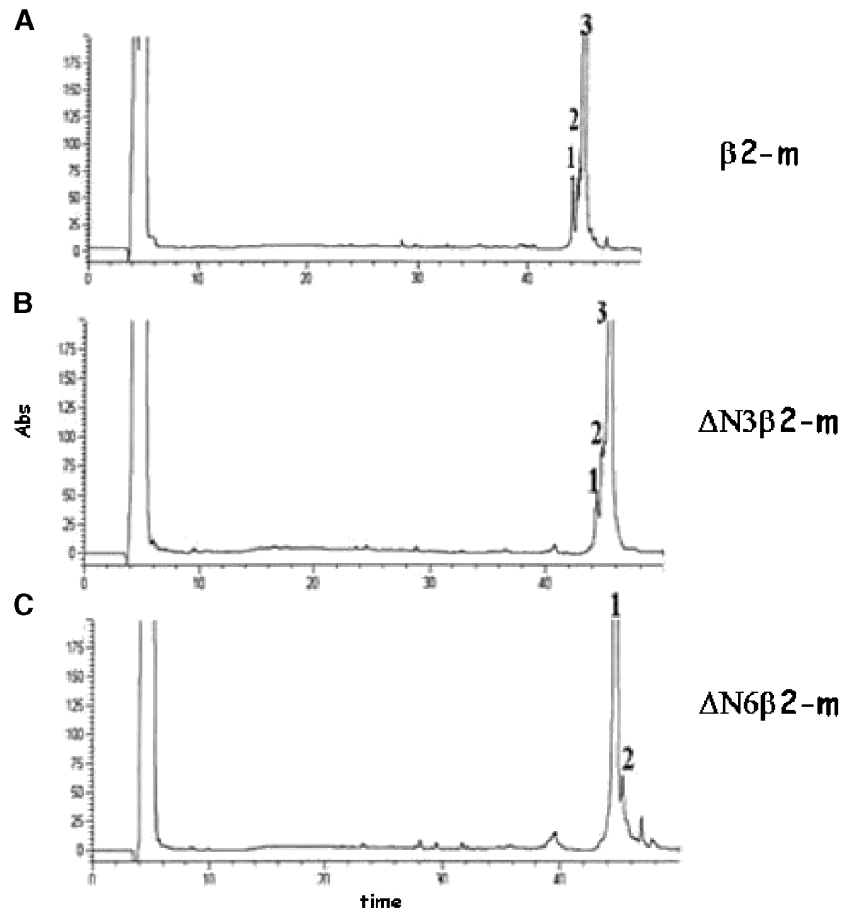
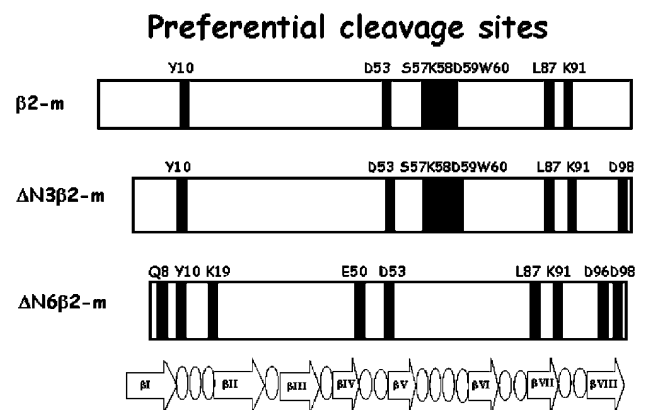


Fig. 3. HPLC analysis of the aliquot withdrawn following 15 min of endoprotease Asp-N incubation of native  $\beta 2\text{-m}$  (A),  $\Delta N3\beta 2\text{-m}$  (B) and  $\Delta N6\beta 2\text{-m}$  (C). The indicated fractions were manually collected and the eluted peptides were identified by ESMS.

occurrence of preferential cleavage sites at Asp53 and Asp59. Nearly identical results were obtained from the digestion experiment carried out on the truncated protein  $\Delta N3\beta 2\text{-m}$  (Fig. 3B). However, a further hydrolysis site was detected at Asp98 as inferred by the presence of the peptides 4–97 (peak 3). Endoprotease Asp-N digestion of  $\Delta N6\beta 2\text{-m}$  (Fig. 3C) required a much lower enzyme-to-substrate ratio compared to  $\beta 2\text{-m}$ , suggesting a higher accessibility of the truncated protein. In common with  $\beta 2\text{-m}$  and  $\Delta N3\beta 2\text{-m}$ ,  $\Delta N6\beta 2\text{-m}$  was readily cleaved at Asp53 but no cleavage was detected at Asp59 even after prolonged digestion times. However, two further hydrolysis sites were identified at Asp96 and Asp98 in the C-terminal region, confirming a higher accessibility of the C-terminus in the truncated proteins.

Similar results were obtained with the other proteolytic enzymes, and the cleavage sites are reported in Scheme 1. In the N-terminal region, the three proteins were cleaved at Tyr10 but only  $\Delta N6\beta 2\text{-m}$  underwent hydrolysis at Gln8 and Lys19, suggesting that its N-terminal region is more disordered than the corresponding region of the parent molecule. A peculiar proteolytic accessibility was observed in the regions of strands V and VI of native  $\beta 2\text{-m}$  and  $\Delta N3\beta 2\text{-m}$  with cleavages occurring at Ser57, Lys58, Asp59 and Trp60 within the loop and at Asp53 in the  $\beta$ -bulge of strand V, i.e., at rather exposed and flexible locations of the parent structure. In  $\Delta N6\beta 2\text{-m}$ ,

only the initial part of strand V underwent hydrolysis (Glu50, Asp53), while the  $\beta$ -bulge, loop and strand VI appear to be protected, suggesting that this region is endowed with less conformational flexibility. Proteolysis at the C-terminus occurred at Leu87 and Lys91 for all proteins, while  $\Delta N3\beta 2\text{-m}$  showed hydrolysis at Asp98 and  $\Delta N6\beta 2\text{-m}$  underwent cleavages at Asp96 and Asp98.



Scheme 1. Schematic representation of the results obtained from limited proteolysis experiments on the soluble forms of native  $\beta 2\text{-m}$  and  $\Delta N6\beta 2\text{-m}$ . Trypsin, endoprotease AspN, endoprotease V8, chymotrypsin, proteinase K and elastase were used as conformational probes.

As a whole, these results indicated that the truncated protein retains part of the structure of the intact  $\beta 2$ -m even though these forms appeared more susceptible to proteolytic digestion than the longer one. A greater flexibility is gained upon the removal of the first six amino acid residues leading to consider  $\Delta N6\beta 2$ -m partially unfolded in comparison to the intact  $\beta 2$ -m and therefore a good example of amyloid intermediate.

### 3.2. Limited proteolysis on fibril of $\beta 2$ -m and $\Delta N6\beta 2$ -m

Limited proteolysis experiments were performed on the insoluble fibrils obtained from both  $\beta 2$ -m and  $\Delta N6\beta 2$ -m using trypsin, chymotrypsin and endoprotease Asp-N as conformational probes, as these enzymes had previously provided informative results on the topology of the soluble proteins. Fibrils were washed accurately before enzyme incubation to remove any possible soluble component. After centrifugation, the recovered pellet was diluted in the working buffer and incubated with each proteolytic enzyme. Aliquots of the reaction mixture were withdrawn at different interval times, treated with 0.4% TFA in 40% acetonitrile to solubilize fibrillar aggregates, and fractionated by HPLC. Individual fractions were then collected and the fibrils-released fragments identified by ESMS analysis.

Fig. 4 shows the HPLC analysis of the aliquots withdrawn following 15 min of endoprotease Asp-N digestion of the fibrils from  $\beta 2$ -m (A) and  $\Delta N6\beta 2$ -m (B). Almost identical chromatographic profiles were obtained that essentially showed the presence of the undigested proteins (fraction 1). However, a protein species exhibiting molecular mass of  $11613.4 \pm 1.0$  Da coeluting with the untouched protein was detected in peak 1. This component was identified as the peptides 1–97, generated

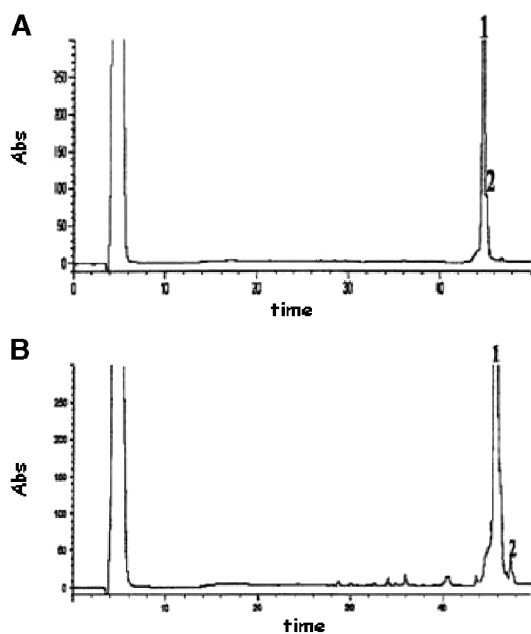


Fig. 4. HPLC analysis of the aliquot withdrawn following 15 min of endoprotease Asp-N incubation of synthetic fibrils from native  $\beta 2$ -m (A) and  $\Delta N6\beta 2$ -m (B). The indicated fractions were manually collected and the eluted peptides were identified by ESMS.

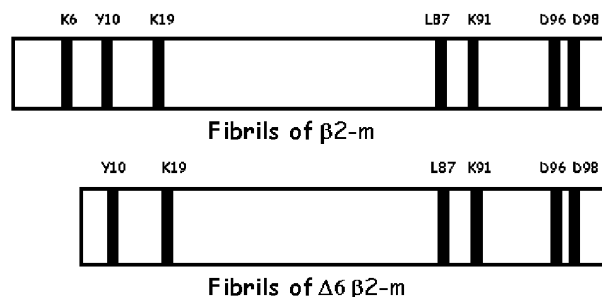


Fig. 5. Schematic representation of the results obtained from limited proteolysis experiments on synthetic fibrils from native  $\beta 2$ -m and  $\Delta N6\beta 2$ -m. Preferential cleavage sites are depicted by solid bars. Trypsin, chymotrypsin and endoprotease Asp-N were used as conformational probes. The integrity of the fibrils was assessed by the Thioflavin assay.

by a proteolytic cleavage at Asp98. In both chromatograms, peak 2 contained the peptides 1–95, indicating the occurrence of a cleavage site at Asp96.

Similar results were obtained when the proteolytic experiments were carried out with chymotrypsin and trypsin. Mass spectral analysis of the HPLC fractions from chymotryptic digestion revealed the presence of the complementary fragments 1–10 (or 7–10 in the case of  $\Delta N6\beta 2$ -m) and 11–99, identifying Tyr 10 as a preferential proteolytic site. A secondary cleavage site was inferred at Leu 87 by the occurrence of the complementary peptide pairs 88–99 and 11–87. Fibrils from both intact  $\beta 2$ -m and truncated  $\Delta N6\beta 2$ -m were immediately cleaved by trypsin in the N-terminal region at Lys 6, releasing the fragments 7–99, and at Lys19 generating the peptides 20–99, and in the C-terminus at Lys91.

The distribution of preferential cleavage sites observed on the fibrils originated from intact  $\beta 2$ -m and  $\Delta N6\beta 2$ -m is reported in Fig. 5. These data clearly indicated that both native  $\beta 2$ -m and truncated  $\Delta N6\beta 2$ -m exhibited an identical distribution of preferential proteolytic sites in the fibrillar form which was nearly superimposable to that observed for the soluble form of  $\Delta N6\beta 2$ -m (see Scheme 1). On the contrary, a totally different pattern of proteolytically accessible sites was identified in the soluble full-length  $\beta 2$ -m. Once inserted in the fibrillar polymer, a large portion of the central region of  $\beta 2$ -m became protected against protease action, whereas a much higher accessibility was observed at the amino- and carboxy-termini. In particular, the region encompassing residues 53–61, which, in the soluble protein, had been easily cleaved at numerous sites (Asp 53, Lys 58, Asp 59, Trp 60 and Ser 61), was found to be completely resistant to proteolysis in the fibrils.

## 4. Discussion

Structural elucidation of proteins in solution is generally achieved by NMR spectroscopy that usually remains plagued by heavy instrumentation requirements, needs a millimolar concentration of a non-aggregating protein solution and, in addition, is of limited success in the detailed analysis of partly folded and fluctuating states of proteins due to resonance broadening and/or lack of sufficient chemical shift dispersion.

Even X-ray crystallography can be utilized for protein structure analysis only if suitable protein crystals are available and, moreover, it is of no use with dynamic protein systems.

Limited proteolysis in combination with mass spectrometric identification of the fragments generated constitutes an alternative and complementary approach to probe protein conformation and dynamics. Under controlled experimental conditions, the preferential cleavage sites along the polypeptide chain are characterized by enhanced backbone flexibility, are generally devoted of stable secondary structure and are not embedded in rigid hydrogen bonding constraints. Local unfolding is most likely required for the proteolytic cleavage of a peptide bond because a large conformational change is needed to accommodate a peptide segment within the active site of a protease [15]. Because of the sensitivity of both proteolytic probes and mass spectrometry, transient intermediates can also be analyzed by this method, which leads to monitor the progression of proteolysis and thereby to gain insight into protein dynamics.

In the investigation of protein conformation, the exposed regions are identified on the basis of subtle differences in the rate of enzymatic hydrolysis to distinguish preferred from protected cleavage sites. Experimental conditions including pH, digestion time and the enzyme to substrate ratio have then to be carefully selected in order to both ensure maximum stability of the protein native conformation and to address proteases activity towards a few well-defined sites. Unfolding of the polypeptide chain would result in enzymatic hydrolyses occurring at random, thus, leading to incorrect assessing of the preferred cleavage sites. The amount of proteases in the reaction mixture can be used to limit to a great extent their activity, even when broad-specificity proteases had to be used. Finally, the enzymatic digestions can be monitored on a time-course basis to enhance discrimination between preferred and protected cleavage sites.

A panel of proteases with different specificities was employed in this study to ensure that the selectivity of the cleavage is not related to, or limited by, the specificity of the enzyme. The accessibility of the side chain of a particular residue and the local flexibility of the polypeptide chain should eventually be the only factors which define whether or not proteolysis can occur at a particular site. The grouping of the preferential cleavage sites within the same region of the protein regardless of the proteases used is strongly indicative of the consistency of the data and suggestive of the exposure of that particular region. The peptide bonds susceptible to protease action and hence the accessible amino acid residues were assigned from the identification of the two complementary peptides released from the intact protein following a single proteolytic event. The determination of their accurate molecular mass leads to the unambiguous identification of the fragments and hence to the assignment of the cleavage sites.

This combined strategy was employed to probe the surface topology and the conformational differences of native  $\beta$ 2-m and the truncated  $\Delta$ N6 $\beta$ 2-m species both in soluble and in the fibrillar forms [16]. The conformation in solution of a further truncated mutant  $\Delta$ N3 $\beta$ 2-m lacking only three residues at the N-terminus was also examined as an intermediate state. The

combination of different proteolytic experiments clearly showed that native  $\beta$ 2-m and  $\Delta$ N3 $\beta$ 2-m shared essentially the same conformation, confirming NMR data [4], with the truncated mutant exhibiting only a slightly higher accessibility in the C-terminal region. On the contrary, significant structural differences exist between the  $\beta$ 2-m and  $\Delta$ N6 $\beta$ 2-m in solution. As a general comment, the removal of the first six residues of  $\beta$ 2-m reduces its folding stability and enhances its susceptibility to proteolytic digestion. Analysis of the respective patterns of preferential proteolytic sites supports a model in which the truncated protein retains part of the structure of the intact  $\beta$ 2-m with major differences located at the end moiety of strand V and subsequent loop with strand VI and at both the N- and C-termini of the protein. In particular, the intact protein showed a higher accessibility at the  $\beta$ -bulge of strand V and within the loop connecting strands V and VI. These results matched remarkably well with a subsequent crystallographic and NMR investigation of native  $\beta$ 2-m. In the solution structure of  $\beta$ 2-m, in fact, the vast majority of the protein adopts a conformation in which the  $\beta$ -bulge of strand V was clearly detected although it was not present in the crystal form of the protein [5].

Proteolytic investigation of  $\Delta$ N6 $\beta$ 2-m demonstrated that the corresponding region in the truncated species was completely resistant to proteases, suggesting the occurrence of local conformational changes. The decrease in conformational accessibility inferred from limited proteolysis seems to indicate the involvement of strand V in intermolecular pairing. These data support the hypothesis lately suggested by Trinh et al. [5] that the long straight conformation of strand V observed in the crystal form of  $\beta$ 2-m could be involved in the initiation of amyloid fibril formation. According to the proposed model of amyloid protofilament formation [17], from its oligomeric state the protein should further polymerize even at physiological pH (at which fibrillogenesis of full-length protein is prevented) to create amyloid fibrils. This suggests that the structure of  $\Delta$ N6 $\beta$ 2-m under the conditions used for the present study could be regarded as an amyloidogenic conformation. Interestingly, point mutations in the N-terminal strands destabilise native  $\beta$ 2-m and results in rapid fibrils formation at neutral pH [18].

A complete different scenario was depicted by the limited proteolysis analysis of synthetic fibrils obtained *in vitro* from intact  $\beta$ 2-m and truncated  $\Delta$ N6 $\beta$ 2-m [19]. An identical distribution of preferential proteolytic sites was observed in both fibrils, which was nearly superimposable to that observed for the soluble form of  $\Delta$ N6 $\beta$ 2-m. In particular, the central region of the protein spanning residues 53–60, which had been easily cleaved in the full-length soluble  $\beta$ 2-m, was fully protected in the fibrillar form. In addition, the amino- and carboxy-terminal regions of  $\beta$ 2-m became exposed to the solvent in the fibrils, whereas they were completely masked in the native protein. These data indicated that synthetic fibrils essentially consists of an unaccessible core comprising residues 20–87 of the  $\beta$ 2-m protein with strands I and VIII being not constrained in the fibrillar polymer and exposed to the proteases. These results are in complete agreement with

NMR H/D exchange experiments showing that many residues located in native loops participate in forming a strong hydrogen bond network in the fibrils, becoming protected from the exchange, whereas the N- and C-terminal ends of the molecule remained non-protected [20].

Finally, proteolytic cleavages observed *in vitro* at Lys 6 and Lys 19 reproduce specific cleavages occurring *in vivo* to generate the truncated forms of  $\beta_2$ -m which have been detected in natural fibrils [21,22]. These cleavages were neither observed in the soluble full-length  $\beta_2$ -m, where the N-terminal region was completely inaccessible to proteases. Therefore, proteolysis at these sites can only take place following large conformational changes of the protein structure such as those occurring in passing from the native soluble conformation to the fibrillar form. These results then suggest that the proteolytic processing leading to the amino-terminal truncated forms of  $\beta_2$ -m might take place only after the protein is constrained within the fibril structure. This hypothesis is further supported by the finding that although the truncated species was identified in *ex vivo* fibrils, yet this fragment was never detected in plasma.

A molecular mechanism for fibril formation in amyloidosis occurring during long-term hemodialysis can then be proposed.  $\beta_2$ -m must lose certain tertiary interactions to self aggregate in a well-ordered fibrillar polymer and a significant conformation transition is required. Partial unfolding of full-length protein could be caused by pH reduction, interaction with dialytical membranes, or hydrostatic pressure created in the dialytical system. These conformational changes generate the partly unfolded intermediate characterized by an amyloidogenic conformation whose overall topologic structure resembles that of the truncated  $\Delta N6\beta_2$ -m form. The transient component is more susceptible to amyloid deposition and originates the accumulation of insoluble material, which, in turn, drives the entire equilibrium toward the formation of fibrils. Once the amyloid deposit tends to accumulate, the extracellular proteases attempt to digest the insoluble material as a repair mechanism. However, the tightly packed structure of the fibril core prevents proteolysis and addresses protease action toward the amino- and carboxy-terminal ends, thus explaining the presence of the amino-terminal truncated forms of  $\beta_2$ -m in natural fibrils.

## Acknowledgements

This study was supported by MIUR (PRIN projects 1999 Cod. 9905108318 and 2002 Cod. 2002058218 and FIRB projects 2001 Cod. RBAU015B47 and Cod. RBNE01S29H 2003 Cod. RBNE03PX83) and Ministero della Sanità: Ricerca finalizzata sulla Malattia di Alzheimer.

## References

[1] C.M. Dobson, Protein misfolding, evolution and disease, *Trends Biochem. Sci.* 24 (1999) 329–332.  
 [2] W.S. Gosal, I.J. Morten, E.W. Hewitt, D. Alastair Smith, N.H. Thomson, S.E. Radford, Competing pathways determine fibril morphology in the

self-assembly of beta(2)-microglobulin into amyloid, *J. Mol. Biol.* 351 (2005) 850–864.  
 [3] G.W. Platt, V.J. McParland, A.P. Kalverda, S.W. Homans, S.E. Radford, Dynamics in the unfolded state of  $\beta_2$ -microglobulin studied by NMR, *J. Mol. Biol.* 346 (2005) 279–294.  
 [4] A. Corazza, F. Pettirossi, P. Viglino, G. Verdone, J. Garcia, P. Dumy, S. Giorgetti, P. Mangione, S. Raimondi, M. Stoppini, V. Bellotti, G. Esposito, Properties of some variants of human  $\beta_2$ -microglobulin and amyloidogenesis, *J. Biol. Chem.* 279 (2004) 9176–9189.  
 [5] C.H. Trinh, D.P. Smith, A.P. Kalverda, S.E.V. Phillips, S.E. Radford, Crystal structure of monomeric human  $\beta_2$ -microglobulin reveals clues to its amyloidogenic properties, *Proc. Natl. Acad. Sci.* 99 (2002) 9771–9776.  
 [6] T. Chiba, Y. Hagihara, T. Higurashi, K. Hasegawa, H. Naiki, Y. Goto, Amyloid fibril formation in the context of full-length protein: effects of proline mutations on the amyloid fibril formation of beta2-microglobulin, *J. Biol. Chem.* 278 (2003) 47016–47024.  
 [7] D.F. Moriarty, D.P. Raleigh, Effects of sequential proline substitutions on amyloid formation by human amylin 20–29, *Biochemistry* 38 (1999) 1811–1818.  
 [8] D.P. Smith, S. Jones, L.C. Serpell, M. Sunde, S.E. Radford, A systematic investigation into the effect of protein destabilisation on beta 2-microglobulin amyloid formation, *J. Mol. Biol.* 330 (2003) 943–954.  
 [9] F. Chiti, N. Taddei, F. Baroni, C. Capanni, M. Stefani, G. Ramponi, C.M. Dobson, Kinetic partitioning of protein folding and aggregation, *Nat. Struct. Biol.* 9 (2002) 137–143.  
 [10] F. Zappacosta, A. Pessi, E. Bianchi, S. Venturini, M. Sollazzo, A. Tramontano, G. Marino, P. Pucci, Probing the tertiary structure of proteins by limited proteolysis and mass spectrometry: the case of minibody, *Protein Sci.* 5 (1996) 802–813.  
 [11] S. Orrù, F. Dal Piaz, A. Casbarra, G. Biasiol, R. De Francesco, C. Steinkuhler, P. Pucci, Conformational changes in the NS3 protease from hepatitis C virus strain BK monitored by limited proteolysis and mass spectrometry, *Protein Sci.* 8 (1999) 1445–1454.  
 [12] F. Gejyo, T. Yamada, S. Odani, Y. Nakagawa, M. Arakawa, T. Kunitomo, H. Kataoka, M. Suzuki, Y. Hirasawa, T. Shirahama, et al., A new form of amyloid protein associated with hemodialysis was identified as b2-microglobulin, *Biochem. Biophys. Res. Commun.* 129 (1985) 701–706.  
 [13] M. Stoppini, P. Arcidiaco, P. Mangione, S. Giorgetti, D. Brancaccio, V. Bellotti, Detection of fragments of b2-microglobulin in amyloid fibrils, *Kidney Int.* 57 (2000) 349–350.  
 [14] V. Bellotti, M. Stoppini, P. Mangione, M. Sunde, C.V. Robinson, L. Asti, D. Brancaccio, G. Ferri,  $\beta_2$ -microglobulin can be refolded into a native state from *ex vivo* amyloid fibrils, *Eur. J. Biochem.* 258 (1998) 61–67.  
 [15] S.J. Hubbard, F. Eisenmenger, J.M. Thornton, Modeling studies of the change in conformation required for cleavage of limited proteolytic sites, *Protein Sci.* 3 (1994) 757–768.  
 [16] G. Esposito, R. Michelutti, G. Verdone, P. Viglino, H. Hernandez, C.V. Robinson, A. Amoresano, F. Dal Piaz, M. Monti, P. Pucci, P. Mangione, M. Stoppini, G. Merlini, G. Ferri, V. Bellotti, Removal of the N-terminal hexapeptide from human beta2-microglobulin facilitates protein aggregation and fibril formation, *Protein Sci.* 9 (2000) 831–845.  
 [17] M. Sunde, L.C. Serpell, M. Bartlam, P.E. Fraser, M.B. Pepys, C.C.F. Blake, Common core structure of amyloid fibrils by synchrotron X-ray diffraction, *J. Mol. Biol.* 273 (1997) 729–739.  
 [18] S. Jones, D.P. Smith, S.E. Radford, Role of the N- and C-terminal strands of  $\beta_2$ -microglobulin in amyloid formation at neutral pH, *J. Mol. Biol.* 330 (2003) 935–941.  
 [19] M. Monti, S. Principe, S. Giorgetti, P. Mangione, G. Merlini, A. Clark, V. Bellotti, A. Amoresano, P. Pucci, Topological investigation of amyloid fibrils obtained from  $\beta_2$ -microglobulin, *Protein Sci.* 11 (2002) 2362–2369.  
 [20] M. Hoshino, H. Katou, Y. Hagihara, K. Hasegawa, H. Naiki, Y. Goto, Mapping the core of the  $\beta_2$ -microglobulin amyloid fibril by H/D exchange, *Nat. Struct. Biol.* 9 (2002) 332–336.  
 [21] R.P. Linke, H. Hampl, H. Lobeck, E. Ritz, J. Bommer, R. Waldherr, M. Eulitz, Lysine-specific cleavage of  $\beta_2$ -microglobulin in amyloid deposits associated with hemodialysis, *Kidney Int.* 36 (1989) 675–681.